Металлофиз. новейшие технол. / *Metallofiz. Noveishie Tekhnol.*
2018, т. 40, № 12, сс. 1573–1587/ DOI: 10.15407/mfint.40.12.1573
Оттиски доступны непосредственно от издателя
Фотокопирование разрешено только
в соответствии с лицензией

PACS numbers: 02.70.Dh, 74.25.nn, 74.72.-h, 74.78.-w, 84.32.-y, 84.40.-x, 85.25.-j

Miniature Meander- and Fractal-Shaped Microstrip Resonators

A. A. Kalenyuk and S. I. Futimsky

G. V. Kurdyumov Institute for Metal Physics, N.A.S. of Ukraine,
36 Academician Vernadsky Blvd.,
UA-03142 Kyiv, Ukraine

Numerical calculations of the characteristics of the meander- and fractal-shape (Hilbert curve) topologies of close-packed microstrip resonators are performed. The amplitude–frequency characteristics, resonance frequencies, quality factors, and geometric factors are calculated. The mechanisms of neighbouring resonator segments' interaction are found. The latter strongly affects both the resonance frequency and the quality factor. Two high-temperature superconducting fractal-shaped microstrip resonators are fabricated using thin films of $YBa_2Cu_3O_{7-\delta}$ (YBCO); the amplitude–frequency characteristics, the resonance frequencies, and the quality factor–frequency dependences are measured. Frequency dependence of a surface resistance of the YBCO film is found. The quality factors of the superconducting and copper resonators are compared, and the reasonability of the YBCO films' usage as a material for thin-film resonators' manufacturing is assessed.

Key words: microwave, high-temperature superconductivity, microstrip resonator, fractal, quality factor, surface resistance.

Проведено чисельний розрахунок характеристик меандрових і фрактальних (Гільбертова крива) топологій щільноупакованих мікросмужкових резонаторів. Розраховано амплітудно-частотні характеристики, резонансні частоти, добротності та геометричні фактори. Знайдено механізми взаємодії сусідніх сеґментів резонатора, які спричиняють сильний вплив на резонансну частоту та добротність. З тонких плівок $YBa_2Cu_3O_{7-\delta}$ (YBCO) було виготовлено два високотемпературних надпровідних фрактальних мікросмужкових резонатора, виміряно їхні амплітудно-частотні харак-

Corresponding author: Aleksey A. Kalenyuk
E-mail: kalenyuk77@gmail.com

Citation: A. A. Kalenyuk and S. I. Futimsky, Miniature Meander- and Fractal-Shaped Microstrip Resonators, *Metallofiz. Noveishie Tekhnol.*, **40**, No. 12: 1573–1587 (2018), DOI: 10.15407/mfint.40.12.1573.

теристики, резонансні частоти та залежності добротности від частоти. Знайдено частотну залежність поверхневого опору плівки YBCO. Проведено порівняння добротностей надпровідних і мідних резонаторів та зроблено оцінку доцільности використання плівок YBCO в якості матеріялу для виготовлення резонаторів.

Ключові слова: мікрохвилі, високотемпературна надпровідність, мікросмужковий резонатор, фрактал, добротність, поверхневий опір.

Проведён численный расчёт характеристик меандровых и фрактальных (кривая Гильберта) топологий плотноупакованных микрополосковых резонаторов. Рассчитаны амплитудно-частотные характеристики, резонансные частоты, добротности и геометрические факторы. Найдены механизмы взаимодействия соседних сегментов резонатора, которые оказывают сильное влияние на резонансную частоту и добротность. Из тонких плёнок $YBa_2Cu_3O_{7-\delta}$ (YBCO) были изготовлены два высокотемпературных сверхпроводящих фрактальных микрополосковых резонатора, измерены их амплитудно-частотные характеристики, резонансные частоты и зависимости добротности от частоты. Найдена частотная зависимость поверхностного сопротивления плёнки YBCO. Проведено сравнение добротностей сверхпроводящих и медных резонаторов и сделана оценка целесообразности использования плёнок YBCO в качестве материала для изготовления резонаторов.

Ключевые слова: микроволны, высокотемпературная сверхпроводимость, микрополосковый резонатор, фрактал, добротность, поверхностное сопротивление.

(Received 27 June, 2018)

1. INTRODUCTION

Modern communication microwave systems require improvement of noise characteristics and limitation of active noise created by other devices. Microwave selective filters based on resonators with a high quality factor are widely used for this purpose. For the frequencies of about a few gigahertz, planar microstrip, coplanar and slot line resonators have proved their advantages for usage. These structures, as compared with cavity resonators, are small in size, simple for manufacturing, and can be easily integrated together with modern basic electronic surface mounted devices (SMD).

For application of planar resonators in microwave monolithic integrated circuits, it is necessary to solve the problems of miniaturization as well as increase of the quality factor. Usage of superconducting materials instead of conventional metals essentially increases the resonator's quality factor and makes it possible to use a minimum number of resonators for constructing superconducting highly-selective filters, whose advantage is small losses in the passband (the influence of the

number of resonators and their quality factors on the losses in the filter passband is considered in detail in [1]).

Linear dimensions of planar resonators can be large, since they are related with the wavelength ≅ 30 cm for the frequency of 1 GHz. Therefore, the task of long resonator placing on a substrate with limited area is quite topical. For this purpose, a meander (zigzag) line is usually used. Increase of filling density creates the problem of neighbouring resonator segments mutual interaction. This makes analytical calculations impossible and forces the usage of numerical methods.

Recent progress of computer technology and development of powerful calculating algorithms made it possible to perform calculations of resonators with complicated topology, for example, fractal-shaped, that possess high filling density over a limited area (close-packed) and ensure good alternative to meander-shaped resonators.

This work is devoted to the study of miniaturization problems of microwave planar topologies using the close-packed meander- and fractal-shaped microstrip resonators as examples.

2. THE RESONANCE FREQUENCY AND EFFECTIVE DIELECTRIC CONSTANT OF MICROSTRIP RESONATOR

The microstrip resonator consists of a dielectric substrate with a thickness H, on the one side of which there is a conducting line of width W, and on the other, a solid conductive coating, which plays the role of a ground plane (see Fig. 1, *a*). Dielectric materials with a small loss tangent and a large dielectric constant ε_r are chosen as the substrate. In the microstrip line, the electromagnetic wave propagates both within the dielectric and outside of it. To simplify the calculations, the microstrip on the dielectric substrate is replaced by an equivalent strip immersed in the dielectric space with a dielectric constant ε_{eff} (see Fig. 1, *b*). One has $\varepsilon_{\text{eff}} \approx \varepsilon_r$ for wide strips ($W >> H$) and $\varepsilon_{\text{eff}} < \varepsilon_r$ for narrow ones ($W \leq H$). By the ratio of ε_r to ε_{eff}, one can esti-

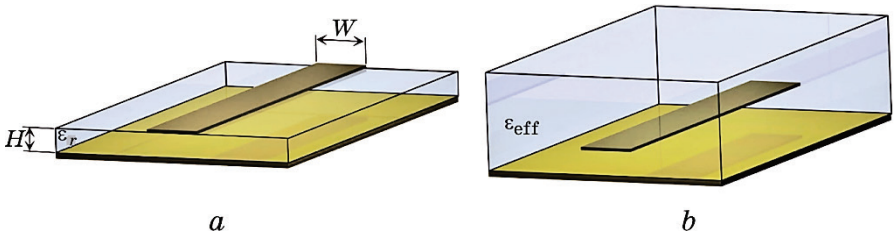

Fig. 1. The microstrip line of width W deposited on a dielectric substrate of thickness H and dielectric constant ε_r (*a*); the equivalent microstrip line within the space filled by dielectric with equivalent dielectric constant ε_{eff} (*b*).

mate what part of the wave propagates outside the dielectric.

For calculation of ε_{eff} value, the approximate analytical expression is used that gives an error $< 1\%$ for $W/H < 1$ [2]:

$$\varepsilon_{\text{eff}} = \frac{\varepsilon_r + 1}{2} + \frac{\varepsilon_r - 1}{2}\left[\frac{1}{\sqrt{1 + 12\left(\frac{H}{W}\right)}} + 0.04\left(1 - \left(\frac{W}{H}\right)\right)^2\right]. \qquad (1)$$

The simplest microstrip resonator with the resonance frequency of first mode F_1 is a straight microstrip line segment with a length $L = \lambda_{\text{eff}} / 2$ (Fig. 2, *a*), where $\lambda_{\text{eff}} = \lambda_0 / \sqrt{\varepsilon_{\text{eff}}}$ is the wavelength in the line, $\lambda_0 = c/F_1$ is the wavelength in a free space, and c is the speed of light.

Based on the foregoing, the first resonance mode frequency is

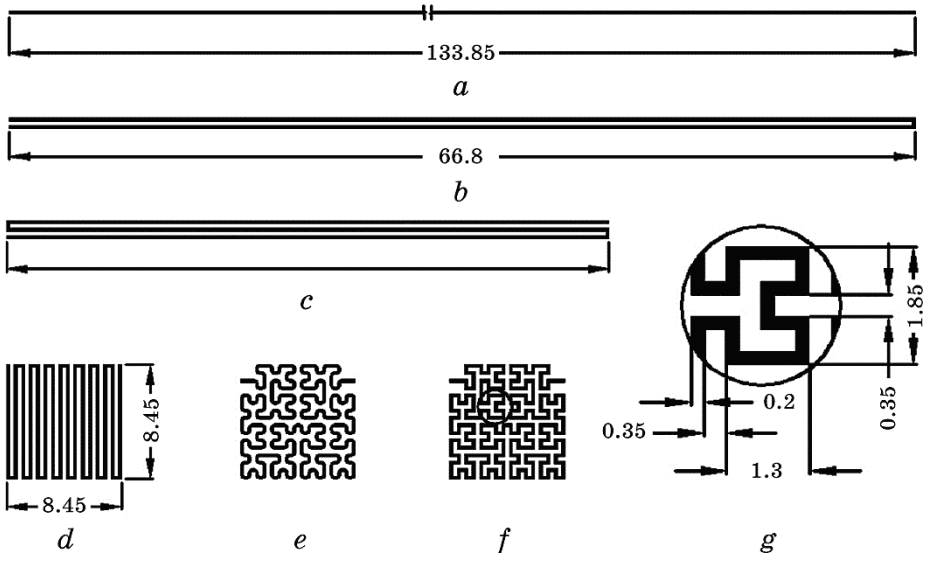

Fig. 2. Topologies of the microstrip meander- and fractal-shaped resonators presented on the same scale: straight resonator M1 (*a*); 'hairpin' or 2 lines meander-shaped resonator M2 (*b*); 3 lines meander-shaped resonator M3 (*c*); 16 lines meander-shaped resonator M16 (*d*); resonators based on fractal Hilbert curve with rounded and orthogonal turns, respectively, (*e*) and (*f*); the enlarged part of the orthogonal fractal-shaped resonator (*g*). All resonators have the line width $W = 0.2$ mm, the physical length $L = 133.85$ mm (with exception of 16 lines meander-shaped resonator with $L = 140.45$ mm, and rounded fractal-shaped resonator with $L = 117.37$ mm), and the distance between adjacent lines 0.35 mm.

$F_1 = \dfrac{c}{2L\sqrt{\varepsilon_{\text{eff}}}}$. The frequencies of following resonance modes, if ε_{eff} is constant, are the multiple to the resonance frequency of first mode:

$$F_n = \frac{nc}{2L\sqrt{\varepsilon_{\text{eff}}}}, \tag{2}$$

where n is the mode number.

In all the subsequent calculations and experiments, we used microstrip lines with width $W = 0.2$ mm, located on substrates with thickness $H = 0.5$ mm and dielectric constant $\varepsilon_r = 10.5$. Substituting these values into the expression (1), we found $\varepsilon_{\text{eff}} = 6.672$. Using the expression (2) and the resonator length value $L = 133.85$ mm, the resonance frequency of first mode, $F_1 = 0.4335$ GHz, was found.

For the complex planar structures containing many turns and interacting sections, the calculation of resonance frequencies by means of analytical expressions is impossible. Therefore, numerical methods such as the method of moments (MoM) are used for this purpose.

The MoM is characterized by the partitioning of x–y plane containing the microstrip line into N cells, followed by the solution of Maxwell equations using the Green functions method [3]. The accuracy of the MoM depends on the cells' size. On the other hand, decrease in the cells' size leads to increase in the number of cells, which strongly affects the calculation time of the topology $t \propto (N^2–N^3)$. The MoM performs calculations within current-carrying planes between dielectric layers. For the entire system, boundary conditions are used in appropriate form for an open space or conducting planes. Thus, the MoM is a quasi-three-dimensional ($2.5D$) algorithm for calculating of fields and currents. Usage of this method assumes the uniformity across the thickness of dielectric layers, which is rather common for planar structures.

In this paper, the calculations of amplitude–frequency characteristics in the quasi-static approximation are performed using the MoM, herewith, the Green's functions are frequency independent. This approach significantly speeds up the calculations and it is justified for the case of small frequencies.

As a result of these calculations, the amplitude–frequency characteristic was obtained from which the resonance frequency of first mode, $F_1 = 0.4322$ GHz, was found. The discrepancy with the analytical calculations was given above 0.3%. The calculations were carried out at the cell size chosen as a compromise between the accuracy and the calculation time needed. A small disagreement of the results suggests that the used cells size is optimal.

Straight microstrips are not suitable for manufacturing of resonators on standard small round or square substrates. Therefore, the to-

pologies with line turns were developed. Such curved lines are called meander lines. The first widely known meander-shaped topology is the 'hairpin-line' containing 2 segments (M2) [4]. This topology allows shortening of the substrate length for more than two times (Fig. 2, *b*). Continuation of the miniaturization led to the development of a meander-shaped three-segment structure (M3) (Fig. 2, *c*). The limiting pattern of the meander-shaped structure for filling of a square (8.45×8.45 mm^2) substrate contains 16 segments (M16) and is shown in Fig. 2, *d*).

Meander-shaped structures contain parallel lengthy segments with electric and magnetic fields, which are interrelated. Such a kind of the mutual interactions makes it impossible to calculate resonance frequencies using simple analytical expressions such as (1) and (2), but these resonance frequencies can be calculated within the context of the theory of long transmission lines using the finite element method (FEM) based on ABCD matrices [5, 6].

Recently, fractal-shaped topologies became popular, for example, those based on Hilbert curves (HC) [7]. HC refer to the curves that fill a restricted plane with a curved line, whose length depends on the iteration number of fractal k, $L = (2^k - 1/2^k)a$, where a is the length of filled square side. By increasing k, it is possible to achieve large values of the resonator length L, with the length limitation being due to the finite width of the microstrip line and the distance between adjacent segments.

Two fractal-shaped Hilbert resonators with the iteration number $k = 4$ are presented in Fig. 2, *e*, *f*. The difference between them consists in the presence of orthogonal (orthogonal fractal-shaped resonator (OF)) (Fig. 2, *f*) or rounded (rounded fractal-shaped resonator (RF)) (Fig. 2, *e*) turns. The ends of the resonators are modernized for the convenience of capacitive coupling supply. For this reason, the length of the resonator OF is less than the length calculated for the Hilbert curve (134.67 mm) and equals to 133.85 mm. Because of roundings, the resonator RF has the length of 117.37 mm. The enlarged fragment of the resonator OF is shown in Fig. 2, *g*. The complex structure of fractal-shaped resonators does not allow the calculations using analytical expressions or the FEM method. In this case, numerical calculations are only possible, for example, using of the MoM.

For close packing of all the resonators (Fig. 2), the distance of 0.35 mm between two adjacent segments was chosen. This size is smaller than the thickness of the substrate and the effect of adjacent segments on each other is significant.

Using the MoM, amplitude–frequency characteristics of first modes of all the resonators were obtained. Copper with thickness of 10 μm and specific conductivity $\sigma = 5.88 \cdot 10^7$ Sm/m was chosen as the strip material. This thickness is much larger than the skin depth at the experi-

ment frequencies.

Comparison of the amplitude–frequency characteristics for the first four modes of the straight M1 and meander-shaped M2 resonators is shown in Fig. 3, *a*. There one can see a shift of the resonator M2 resonance frequencies with respect to the resonance frequencies of the resonator M1, wherein odd modes have a higher frequency while even modes have smaller frequency. Thus, the periodicity of frequency shift equals to two. A similar dependence was observed for the resonator M3 with a periodicity equal three.

The voltage distribution along the resonator length for the first and second modes is shown in Fig. 3, *b*, *c*. On the first resonance mode, the voltage at the ends of the resonator is opposite in sign. On the second mode, the voltage signs coincide. The resonator M2 consists of two closely spaced strongly coupled segments. The voltage sign on the neighbouring parts of the segments is opposite for odd modes and similar for even modes. Therefore, there is an interaction of neighbouring parts of segments in two essentially different regimes: for odd and even modes. In the case of odd mode, the part of electric fields is not closed to the lower ground plane, but to the adjacent line (Figs. 3, *b*, *c*).

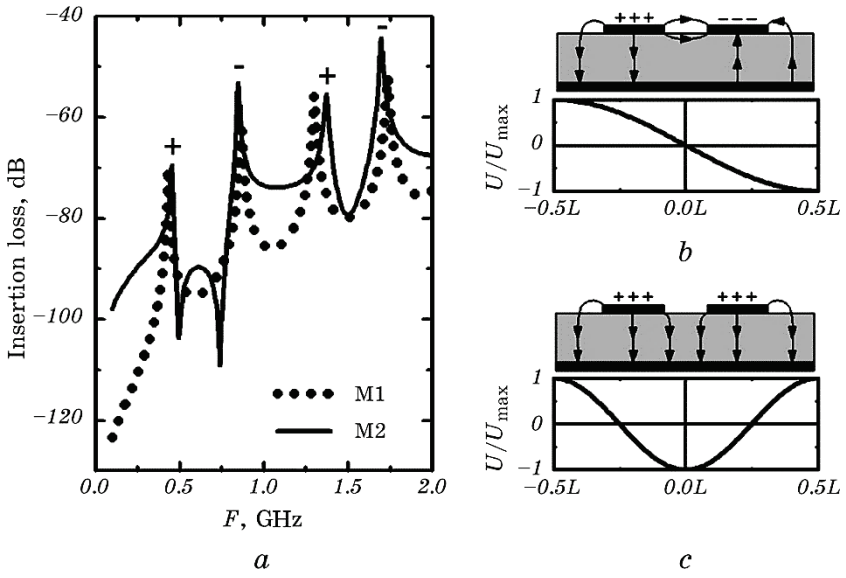

Fig. 3. Amplitude–frequency characteristics of first four resonance modes for resonators M1 and M2 (*a*). The signs '+' and '–' correspond to the resonance frequencies shift of the resonator M2 with respect to the resonator M1 resonance frequencies (*a*). The voltage distribution along the resonator length L for the first (*b*) and second (*c*) resonance modes. In the insets, the electric fields distributions of two closely spaced microstrip lines are shown for odd (*b*) and even (*c*) modes of resonator M2.

This leads to the partial expulsion of electric field from the dielectric to the space above the line and, as a result, to a decrease of ε_{eff} and an increase of resonance frequency in accordance with expression (2). For even modes, there is an opposite process: retraction of the electric field into the dielectric.

For resonator M3, there is an interaction between all three segments. There is a mixed regime on the first and second modes, and an even regime on the third mode.

From the amplitude–frequency characteristics, resonance frequencies F_n were found for all the resonators. Using formula (2), the dependences $\varepsilon_{\text{eff}}(F_n)$ are obtained. The frequency dependencies of $\varepsilon_{\text{eff}}(F_n)$ for the resonators M2 and M3 are shown in Fig. 4, *a*. Periodic variation of ε_{eff} is observed, associated with the switching from odd to even mode of coupling of above-described neighbouring resonator segments. In the resonator M2 for odd modes, the dielectric constant is ε_{eff} (odd) = = 5.927, and for even ones, the dielectric constant is odd (even) = = 7.026. This leads to the existence of an odd mode with the number p, for which the resonance frequency will be greater than the frequency of the next even mode $p + 1$ ($F_p > F_{p+1}$). It is easy to show from Eq. (2)

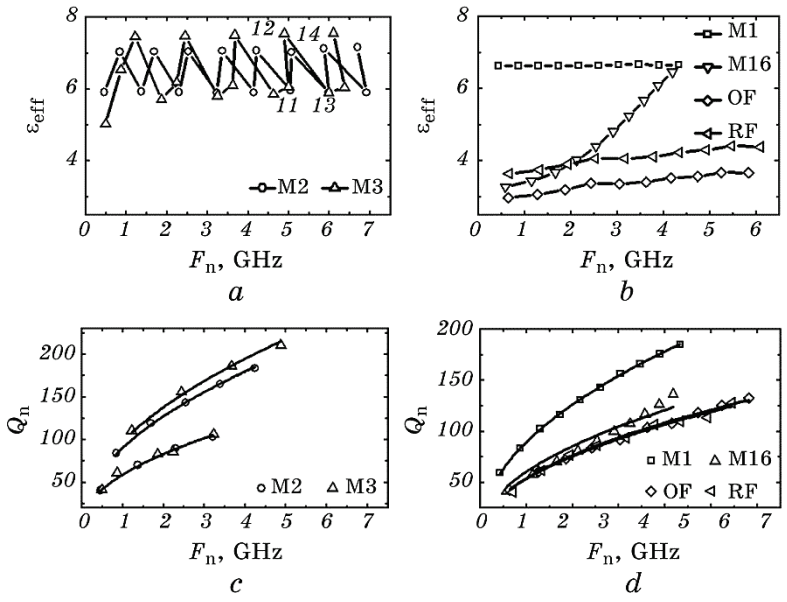

Fig. 4. Frequency dependences of the effective dielectric constant ε_{eff} (*a*, *b*) and the quality factor Q (*c*, *d*) on resonance frequencies for microstrip resonators. As a material for the microstrip fabrication, the copper with a thickness of 10 μm and $\sigma = 5.88 \cdot 10^7$ S/m, and a substrate with $\varepsilon_r = 10.5$ were chosen.

that $p > \left(\sqrt{\frac{\varepsilon_{\text{eff}}(\text{even})}{\varepsilon_{\text{eff}}(\text{odd})}} - 1 \right)^{-1}$. Calculation shows that $p > 11.26$; therefore $F_{13} > F_{14}$. This effect is observed for the resonators M2 (modes 13, 14) and M3 (modes 11, 12) (Fig. 4, *a*).

The length of segments of the resonator M16 is substantially smaller than for the resonators M2 and M3. Therefore, a mixed type of coupling is realized with a change in the proportion of the contribution from the odd to the even regime of interaction with the increase of the mode number. This leads to a progressive increase of ε_{eff} with increasing the frequency (Fig. 4, *b*).

Fractal-shaped resonators, in contrast to meander-shaped resonators, do not have close lengthy parallel sections (Fig. 2, *e*, *f*), and the relation between F_n and ε_{eff} is much weaker than for meander-shaped resonators (Fig. 4, *b*).

3. QUALITY AND GEOMETRIC FACTORS OF A MICROSTRIP RESONATOR

If there are no dielectric and radiation losses, the quality factor of the resonator can be determined from the ratio of magnetic field components in the volume (V) to the field components in the conducting line (S) [8]:

$$Q_n = \frac{2\pi F_n \mu}{R_s} \frac{\int_{\text{resonator}} |H|^2 dV}{\int_{\text{conductor}} |H|^2 dS} = \frac{\Gamma}{R_s}, \tag{3}$$

where Γ is the geometric factor of the resonator, and R_s is the surface resistance of the microstrip line material. For ordinary metals,

$$R_s(F_n) = \sqrt{\frac{\pi F_n \mu_0}{\sigma}}, \tag{4}$$

where σ is the conductivity of the metal.

From Eqs. (3) and (4), it follows that the quality factor of a metal resonator is proportional to $\sqrt{F_n}$.

The results of calculating the quality factor of the copper resonators are shown in Fig. 4, *c*, *d*. The resonator M1 exhibits a quality factor increase: $Q_n \propto \sqrt{F_n}$. For the resonator M2, a periodic change in the quality factor is observed. Dependences $Q_n \propto \sqrt{F_n}$ are noted separately for the groups of even and odd modes. The quality factor for even modes is 50% greater than that for odd ones. Even modes of the resonator M2 have values of quality factors close to that for the resonator M1 (Fig. 4, *d*).

In the resonator M3, each third mode is in the even regime, and it

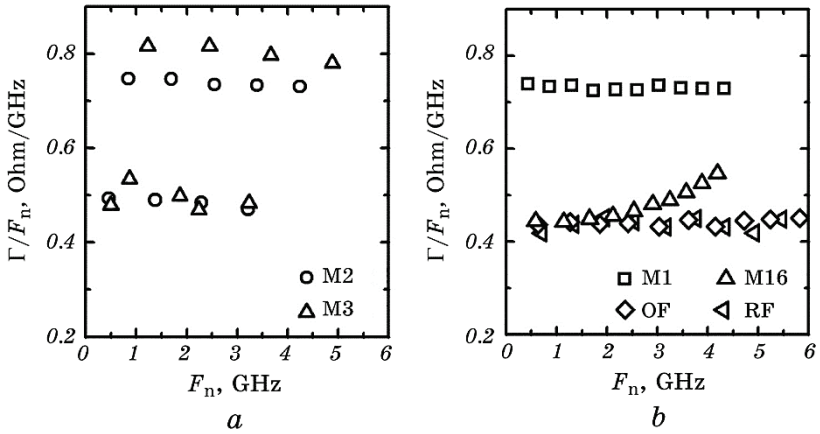

Fig. 5. Comparison of the geometric factors Γ/F_n normalized by the resonant frequency for M2 and M3 resonators (*a*), M16, OF and RF resonators (*b*).

demonstrates quality factors slightly larger than the ones of a straight resonator. The quality factors in the mixed regimes (1, 2, 4, 5, ... modes) are lower than in the even regime by 64%.

Fractal-shaped resonators have shown close frequency dependencies of quality factors, which are described by the function $Q_n \propto \sqrt{F_n}$. The values of a quality factor of fractal-shaped resonators are less by 65% than for the resonator M1 and are commensurable with the ones for the resonator M3 in the mixed coupling regime.

A smooth change of the coupling regime with the frequency for the resonator M16 does not provides a possibility to distinguish groups with identical regimes and describe the quality factor by the dependence $Q_n \propto \sqrt{F_n}$ (Fig. 4, *d*).

The results of calculation for the geometric factor Γ/F_n normalized to the frequency for all types of resonators are presented in Fig. 5. These values are obtained from the frequency dependences of the quality factors (Fig. 4, *c*, *d*) and expressions (3), (4). The resonator M1 and the resonators M2 and M3 operating in the even mode reveal a high value of $\Gamma/F_n > 0.7$ Ohm/GHz. Fractal-shaped resonators M2 and M3 operating in the odd mode and in the mixed mode respectively demonstrate a value of $\Gamma/F_n < 0.5$ Ohm/GHz. The value of Γ/F_n can be taken as a constant for each type of resonator (with the exception of M16) within the same coupling mode of the segments.

4. SUPERCONDUCTING FRACTAL-SHAPED RESONATORS

Two fractal-shaped resonators were fabricated using thin 200 nm $YBa_2Cu_3O_{7-\delta}$ (YBCO) films produced by pulse-laser deposition tech-

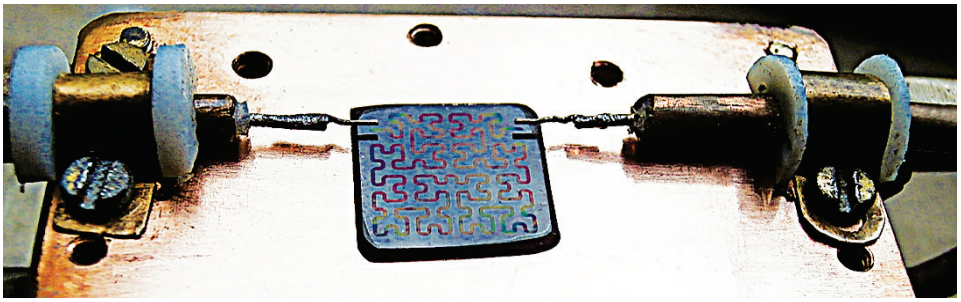

Fig. 6. Fractal-shaped superconducting resonator fabricated and placed on a copper base with adjustable capacitive couplings.

nique (PLD) on sapphire substrates with a subsequent usage of a standard photolithography and etching by argon ions. Subsequently, the resonators were fixed on a copper base, where adjustable coupling antennas were also mounted (Fig. 6). The copper base was placed in a cryostat with a temperature of 80 K. The amplitude–frequency characteristics of fractal-shaped resonators were obtained using the vector analyser of high-frequency circuits.

The results of measured YBCO amplitude–frequency characteristics together with calculated ideal ($R_s = 0$) characteristics of fractal-shaped resonators for the first 5 resonance modes are shown in Fig. 7, *a*. One can see a good agreement of resonance peaks for the measured and calculated characteristics. A discrepancy of the amplitude–frequency characteristics between resonance modes can be explained by the presence of a nonideal (in contrast to the calculation) surrounding space.

The results of measurements of fractal-shaped resonators quality factor are shown in Fig. 7, *b*. Because of highly nonlinear dependence of the quality factor of YBCO resonators on the supplied microwave power [10–12], the measurements were carried out at the minimum power $P_{\text{out}} = -37$ dBm, at which it was possible to extract the resonance peaks from the noise. For both resonators operating on the first mode, the quality factor was greater than 11000 that is about 280 times greater than the calculated quality factor for the copper analogues. With an increase of the resonance mode number, the quality factor decreased strongly and was slightly higher than 6000 for the fifth resonance mode (3.048 GHz).

Using the previously calculated geometrical factors Γ for each mode of the resonator OF (Fig. 5, *b*) and applying formula (3), the frequency dependences of the surface resistance $R_s(F_n)$ of the YBCO film were found (Fig. 7, *c*).

In the context of the two-fluid model, the surface resistance of a thin ($\lambda >> d$) superconducting film R_{sTF} is determined by the formula as follows [8, 9]:

$$R_{sTF}(F_n) = \frac{(2\pi F_n \mu_0)^2 \lambda^4 \sigma_1}{2d} = kF_n^2, \tag{5}$$

where λ is the London penetration depth of the magnetic field in the superconductor, d is the film thickness, and σ_1 is the conductivity of the normal component of electron fluid. During the deposition, a disordered layer [13] arises between the substrate and the film, which adds to the surface resistance an additional contribution leading to the residual resistance R_{s0}:

$$R_s(F_n) = R_{sTF}(F_n) + R_{s0}. \tag{6}$$

Approximation of frequency dependence of the surface resistance by the use of formulas (5), (6) is shown in Fig. 7, *c*. From this approximation, the frequency coefficient $k = 2.187 \cdot 10^{-23}$ and the residual surface resistance $R_{s0} = 20.5$ μΩ were found. Now, the value σ_1 can be estimated. As a parameter λ, the value of 570 nm was chosen [14]. From the value of k, we can find the conductivity of the normal component $\sigma_1 = 1.33$ MSm/m. The value found is close to the value of 1.75 MSm/m, which was obtained in [15].

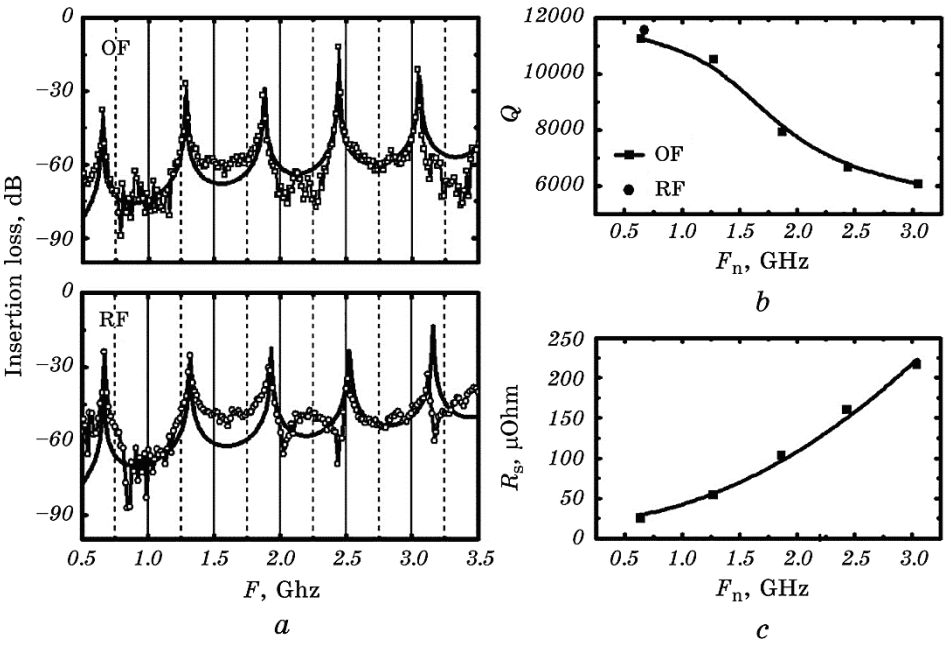

Fig. 7. Calculated and measured amplitude–frequency characteristics of fractal-shaped resonators (*a*); quality factor Q and surface resistance R_s dependences on the resonance mode frequency for the YBCO resonator OF (*b*).

The surface resistance of normal metals increases with a frequency growth as $R_s \propto \sqrt{F}$ (4), and for superconductors (in the framework of the two-fluid model), as $R_s \propto F^2$ (5). On the other hand, the resonator geometric factor is proportional to the frequency: $\Gamma \propto$ F (3). This leads to the frequency dependence of the quality factor for metallic resonators $Q \propto \sqrt{F}$, and for superconducting ones, $Q \propto 1/F$. Consequently, there is an upper limiting frequency F_{up}, for which the values of the surface resistance of a normal-metal resonator and a superconducting resonator become equal (R_s(Cu)/R_s(YBCO) = 1). Above this frequency, there is no sense to use a superconductor as a material for increasing the quality factor of resonators. Using the approximated frequency dependence of the surface resistance of the YBCO film (Fig. 7, *c*) and frequency dependence of the surface resistance of the copper film (Eq. (4)), the limiting frequency F_{up} = 52 GHz was found (Fig. 8, *a*). In the work [13], surface resistance measurements were described; they showed an excess of the surface resistance of similar YBCO films over the surface resistance of copper at frequency of 65 GHz, which agrees well with the result of F_{up} estimation.

In the low-frequency range, limitations on the usage of YBCO films are related to the existence of a residual resistance R_{s0}. Using the frequency dependence for the copper surface resistance (Eq. (4)) and the residual resistance with value for the YBCO film R_{s0} = 20.5 μΩ found above, the lower limiting frequency F_{low} = 6.5KHz was calculated (Fig. 8, *a*). The calculated range F = 6.5 KHz–52 GHz of advisability to change copper resonators by YBCO resonators completely covers the range of microstrip transmission lines usage (≅ 0.3 GHz–20 GHz). But it should be taken into account that the ratio of the copper surface resistance to the surface resistance of YBCO falls rapidly with the frequency increase, and for the criterion R_s(Cu)/R_s(YBCO) > 100, the up-

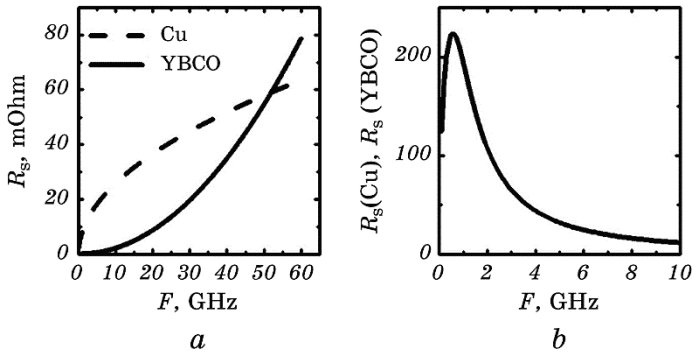

Fig. 8. Frequency dependences of the surface resistance for superconducting (YBCO) and copper films (*a*); frequency dependence of the criterion R_s(Cu)/R_s(YBCO) (*b*).

per frequency limit falls down to the value of $F_{up100} = 2$ GHz (Fig. 8, *b*) for the YBCO films investigated. An increase in the limiting frequency can be achieved by lowering the temperature from 80 to 20 K. In this case, the surface resistance of the YBCO film falls by more than 100 times [17].

5. CONCLUSION

The paper considers the meander- and fractal-type close-packed microstrip resonators, whose distinctive feature is close arrangement of segments, resulting in a strong interaction between them. Such resonators operating on different resonance modes are in different coupling regimes leading to different microwave field geometry, and, as a consequence, effect on the geometric and quality factors of the resonator. The field configuration change from mode to mode for fractal-shaped resonators manifests itself essentially less than for meander-shaped resonators. This is due to the presence of very short segments of fractal curve compared to the meander one. This property allows us to use a single normalized geometric factor for determination of the surface resistance in a wide frequency range. The calculated geometric factors of resonators made it possible to find frequency dependence of the surface resistance for YBCO film, which could be described in the framework of simple two-fluid model with addition of a residual resistance. Based on proposed model, the reasonability of YBCO films' application as a material for the microstrip resonators' manufacturing is shown.

The authors are grateful to Dr. A. L. Kasatkin for the productive discussion of the results of this work.

This work has been partially supported by the Targeted Research & Development Initiatives Programme funded by the STCU and the National Academy of Science of Ukraine (Project No. 6250).

REFERENCES

1. J.-S. Hong and M. J. Lancaster, *Microstrip Filters for RF/Microwave Applications* (New York, USA: John Wiley & Sons, Inc.: 2001).
2. D. M. Pozar, *Microwave Engineering* (Castleton, NY, USA: JohnWiley & Sons, Inc.: 2012).
3. D. G. Swanson, J. Wolfgang, and J. R. Hoefer, *Microwave Circuit Modeling Using Electromagnetic Field Simulation* (Boston, USA: Artech House, Inc.: 2003).
4. E. G. Cristal and S. Frenkel, *IEEE Trans. Microwave Theory Tech.*, **20**, No. 11: 719 (1972).
5. G. Matthaei, L. Young, and E. M. T. Jones, *Microwave Filters, Impedance-Matching Networks, and Coupling Structures* (New York, USA: McGraw-Hill,

Inc.: 1964), p. 1096.
6. A. A. Kalenyuk, *Low Temp. Phys.*, **35**, No. 2: 105 (2009).
7. H.-X. Xu, G.-M. Wang, C.-X. Zhang, and J.-G. Liang, *Int. J. RF Microwave Comput.-Aided Eng.*, **21**, No. 4: 399 (2011).
8. M. J. Lancaster, *Passive Microwave Device Applications of High-Temperature Superconductors* (New York, USA: Cambridge University Press: 1997).
9. I. B. Vendik, *Supercond. Sci. Technol.*, **13**, No. 7: 974 (2000).
10. A. A. Kalenyuk, A. L. Kasatkin, and V. M. Pan, *Proc. of Symp. 'The 6th International Kharkov Symposium on Physics and Engineering of Microwaves, Millimeter and Submillimeter Waves–MSMW'07' (June 25–30, 2007)* (Kharkiv: 2007), vol. **1**, p. 413.
11. A. A. Kalenyuk, A. I. Rebikov, A. L. Kasatkin, and V. M. Pan, *Proc. of Symp. '2010 International Kharkov Symposium on Physics and Engineering of Microwaves, Millimeter and Submillimeter Waves–MSMW'2010' (June 21–26, 2010)* (Kharkiv: 2010), p. 1.
12. N. T. Cherpak, A. A. Lavrinovich, A. A. Kalenyuk, V. M. Pan, A. I. Gubin, V. Khramota, A. A. Kurakin, and S. A. Vitusevich, *Telecommun. Radio Eng.*, **69**, No. 15: 1357 (2010).
13. V. L. Svetchnikov, V. S. Flis, A. A. Kalenyuk, A. L. Kasatkin, A. I. Rebikov, V. O. Moskaliuk, C. G. Tretiatchenko, and V. M. Pan, *J. Phys.: Conf. Ser.*, **234**, No. 1: 012041 (2010).
14. V. M. Pan, A. A. Kalenyuk, A. L. Kasatkin, O. M. Ivanyuta, and G. A. Melkov, *J. Supercond. Novel Magn.*, **20**, No. 1: 59 (2007).
15. A. Porch, D. W. Huish, A. V. Velichko, M. J. Lancaster, J. S. Abell, A. Perry, and D. P. Almond, *IEEE Trans. on Appl. Supercond.*, **15**, No. 2: 3706 (2005).
16. V. F. Tarasov, I. V. Korotash, V. M. Pan, M. A. Skoryk, M. Lorenz, S. I. Futimsky, and A. A. Filimonov, *Metallofiz. Noveishie Tekhnol.*, **24**, No. 3: 313 (2002).
17. V. M. Pan, D. A. Luzhbin, A. A. Kalenyuk, A. L. Kasatkin, and V. A. Komashko, *J. Low Temp. Phys.*, **31**, No. 3: 254 (2005).